



**HAL**  
open science

## Magnetic order in the frustrated Ising-like chain compound Sr<sub>3</sub>NiIrO<sub>6</sub>

Emilie Lefrançois, Laurent C. Chapon, Virginie Simonet, Pascal Lejay, Dmitry Khalyavin, Sudhindra Rayaprol, E. V. Sampathkumaran, Rafik Ballou, D.T. Adroja

► **To cite this version:**

Emilie Lefrançois, Laurent C. Chapon, Virginie Simonet, Pascal Lejay, Dmitry Khalyavin, et al..  
Magnetic order in the frustrated Ising-like chain compound Sr<sub>3</sub>NiIrO<sub>6</sub>. 2014. hal-00960753v1

**HAL Id: hal-00960753**

**<https://hal.science/hal-00960753v1>**

Preprint submitted on 18 Mar 2014 (v1), last revised 6 Jun 2014 (v2)

**HAL** is a multi-disciplinary open access archive for the deposit and dissemination of scientific research documents, whether they are published or not. The documents may come from teaching and research institutions in France or abroad, or from public or private research centers.

L'archive ouverte pluridisciplinaire **HAL**, est destinée au dépôt et à la diffusion de documents scientifiques de niveau recherche, publiés ou non, émanant des établissements d'enseignement et de recherche français ou étrangers, des laboratoires publics ou privés.

# Magnetic order in the frustrated Ising-like chain compound $\text{Sr}_3\text{NiIrO}_6$

E. Lefrançois,<sup>1,2,\*</sup> L. C. Chapon,<sup>1</sup> V. Simonet,<sup>2</sup> P. Lejay,<sup>2</sup> D. Khalyavin,<sup>3</sup>  
S. Rayaprol,<sup>4</sup> E. V. Sampathkumaran,<sup>5</sup> R. Ballou,<sup>2</sup> and D. T. Adroja<sup>3,6,†</sup>

<sup>1</sup>*Institut Laue Langevin, 6 rue Jules Horowitz, BP 156, 38042 Grenoble, France*

<sup>2</sup>*Institut Néel, CNRS & Univ. Grenoble Alpes, 25 rue des Martyrs, BP 166, 38042 Grenoble, France*

<sup>3</sup>*ISIS Facility, STFC, Rutherford Appleton Laboratory,  
Chilton, Oxfordshire OX11 0QX, United Kingdom*

<sup>4</sup>*UGC-DAE CSR, Mumbai Center, R-5 Shed, BARC, Trombay, Mumbai 400085, India*

<sup>5</sup>*Tata Institute of Fundamental Research, Homi Bhabha Road, Colaba, Mumbai 400005, India*

<sup>6</sup>*Physics Department, University of Johannesburg,  
PO Box 524, Auckland Park 2006, South Africa*

(Dated: March 19, 2014)

We have studied the field and temperature dependence of the magnetization of single crystals of  $\text{Sr}_3\text{NiIrO}_6$ . These measurements evidence the presence of an easy axis of anisotropy and two anomalies in the magnetic susceptibility. Neutron powder diffraction realized on a polycrystalline sample reveals the emergence of magnetic reflections below 75 K with magnetic propagation vector  $\mathbf{k} = (0, 0, 1)$ , which remained undetected in previous studies. The controversial nature of the two magnetic anomalies common in this family of material is discussed.

PACS numbers: 75.25.-j, 75.30.Cr, 75.30.Gw, 75.47.Lx

## I. INTRODUCTION

In the last decades, the oxides of the family  $\text{A}_3\text{MM}'\text{O}_6$  (A = alkaline-earth metal, M, M' = transition metal) attracted a lot of attention because of their unconventional magnetic properties due to the interplay between low dimensionality, magnetic frustration and magnetocrystalline anisotropy. In these compounds, the magnetic sublattice consists of chains arranged on a triangular lattice. The M and M' ions, on trigonal and octahedral sites respectively, alternate on each chains. In the Heisenberg classical limit, the magnetic ground state for nearest-neighbor antiferromagnetic interchain interaction on a triangular lattice is the  $120^\circ$  spin configuration. More generally in the present systems, the ground state is an incommensurate structure with a pitch determined by the relative strengths of the intrachain and interchain interactions<sup>1</sup>. In the Ising limit however, the frustration is not released and magnetic structures with modulated moments may be stabilized at finite temperature. In particular, in the  $J_1/J_2$  model on a triangular lattice, a partially disordered magnetic configuration system with only two thirds of the chains that order simultaneously has been predicted<sup>2</sup> and observed experimentally in  $\text{CsCoCl}_3$  for instance<sup>3</sup>. The most studied compound in the frustrated regime is  $\text{Ca}_3\text{Co}_2\text{O}_6$  because of its large easy-axis anisotropy which confines the moment along the chain axis. This system famously displays steps in the magnetization below a certain freezing temperature of 10 K. Although the origin of these steps is still a matter of debate, it is certainly a direct consequence of the strong anisotropy which stabilizes two competing magnetic states, an amplitude modulated phase with wave-vector  $\mathbf{k} = (0, 0, 1.01)$  and a commensurate antiferromagnetic phase<sup>4</sup>.

More recently, the attention has been directed towards

analog compounds containing transition metal ions of the 4d and 5d series, with the objective of studying the unconventional magnetic properties of these frustrated systems in the strong spin-orbit regime. Magnetic measurements show that  $\text{Ca}_3\text{CoRhO}_6$ <sup>5</sup>,  $\text{Sr}_3\text{CoIrO}_6$ <sup>6</sup>,  $\text{Sr}_3\text{NiRhO}_6$ <sup>7</sup> and  $\text{Sr}_3\text{NiIrO}_6$ <sup>6,8,9</sup> have a similar behavior to  $\text{Ca}_3\text{Co}_2\text{O}_6$  with two magnetic anomalies at  $T_1$  (90, 90, 45 and 80 K respectively) and  $T_2$  (35, 25, 15 and 15 K respectively), revealed in the magnetic susceptibility. Below  $T_1$ , a deviation from the Curie-Weiss behavior is observed followed by a steep increase in the susceptibility and the onset of strong spin dynamics. This dynamic gets frozen at  $T_2$ . The susceptibility measured after a zero-field cooling is much smaller below this temperature than after a finite field cooling. Whilst the transition temperatures are considerably higher than for  $\text{Ca}_3\text{Co}_2\text{O}_6$ , it appears that the magnetic behavior does not depend on the nature of the exchange interactions, since the first (last) two have intrachain ferromagnetic (antiferromagnetic) interactions. It is relatively surprising to find such similarities in the series, as one would naturally expect a gradual change from localized magnetism in the case of insulating 3d compounds to a magnetic behavior reminiscent of metals for the 5d case. It has been recently shown from ab-initio calculations that for the Ir-based compound  $\text{Sr}_3\text{NiIrO}_6$ , the strong spin-orbit coupling opens a gap in the electronic spectrum<sup>10-12</sup> that may explain the localized magnetism even in the 5d case. This result seems corroborated by neutron powder diffraction experiments on  $\text{Ca}_3\text{CoRhO}_6$  and  $\text{Sr}_3\text{CoIrO}_6$ , which evidenced long-range magnetic ordering below  $T_1$ <sup>6,13</sup> with localized moments on the Co and Rh (Ir) sites. In both cases, the magnetic structure with wave-vector  $\mathbf{k} = (0, 0, 1)$  is compatible either with a partially disordered antiferromagnetic state, i.e. two-thirds of the chains are ordered and antiferromagnetically coupled while one-third remains disordered or with an

amplitude-modulated antiferromagnetic structure.

In this article, we study the magnetic properties of the  $\text{Sr}_3\text{NiIrO}_6$  compound. We report magnetization measurements on single crystals to probe in details the magnetocrystalline anisotropy by applying magnetic field along different crystallographic directions, which was impossible to quantify from previous data obtained on polycrystalline materials. The nature of the magnetic ground state is investigated from neutron powder diffraction measurements as a function of temperature. We propose a model for the magnetic structure compatible with symmetry analysis and discuss the results obtained in comparison with the other compounds of the same family ( $M = \text{Ni}, \text{Co}$  and  $M' = \text{Rh}, \text{Ir}, \text{Co}$ ).

## II. EXPERIMENTAL

Single crystals of  $\text{Sr}_3\text{NiIrO}_6$  were grown using the flux method previously described for the isostructural compound  $\text{Sr}_3\text{NiPtO}_6$ <sup>14</sup>. The high purity starting materials were  $\text{SrCO}_3$ ,  $\text{NiO}$ ,  $\text{Ir}$  and  $\text{K}_2\text{CO}_3$  as solvent. The mixture was heated under air at a rate of  $60^\circ\text{C/h}$  to  $1050^\circ\text{C}$ , held at that temperature for 72 h and ramped to  $880^\circ\text{C}$  at  $6^\circ\text{C/h}$ . The furnace was then naturally cooled down to room temperature. Crystals of hexagonal shape with typical dimension of  $0.8 \times 0.8 \times 0.3 \text{ mm}^3$ , were separated from the remaining  $\text{K}_2\text{CO}_3$  flux using distilled water. Powder samples were also prepared by solid state reaction in order to perform neutron powder diffraction. Details of polycrystalline sample preparation were similar to that given in Ref. 6

The temperature and field dependence of the single-crystal magnetization were measured using a Quantum Design MPMS<sup>®</sup> SQUID magnetometer. The temperature dependence was measured both in zero-field-cooled (ZFC) and field-cooled (FC) mode between 2 and 300 K. In the ZFC protocol, the sample is cooled down to 2 K in zero magnetic field and the magnetization is measured in 0.01 T while heating. In the FC protocol, the sample is cooled down in 0.01 T. The magnetization field dependence was measured in a magnetic field up to 5 T.

Neutron powder diffraction experiments were performed on polycrystalline sample of  $\text{Sr}_3\text{NiIrO}_6$  at the ISIS pulsed neutron source of the Rutherford Appleton Laboratory, U.K. The powder was loaded into a 6 mm diameter vanadium can inserted in a cryostat. High-resolution data were collected on heating between 2 and 100 K, on the WISH diffractometer on the Target Station 2. Rietveld refinements were carried out using the FULLPROF program<sup>15</sup>.

## III. RESULTS

### A. Crystal structure of $\text{Sr}_3\text{NiIrO}_6$

$\text{Sr}_3\text{NiIrO}_6$  crystallizes in the space group  $R\bar{3}c$ . The lattice parameters refined from our neutron data at 100 K,  $a = 9.6095(2) \text{ \AA}$  and  $c = 11.1654(8) \text{ \AA}$ , are consistent with previous results<sup>8</sup>. The crystal structure (see Fig. 1) consists of chains aligned along the  $\mathbf{c}$  direction, formed by alternating face-sharing  $\text{NiO}_6$  trigonal prisms and  $\text{IrO}_6$  octahedra. The chains are distributed on a triangular lattice in the  $(\mathbf{ab})$  plane. The Ir atom occupies the Wyckoff site 6b (0, 0, 0), i.e. there are two Ir in the primitive unit at (0, 0, 0) and  $(0, 0, \frac{1}{2})$ . The Ni atom occupies the Wyckoff site 6a  $(0, 0, \frac{1}{4})$ , generating two Ni in the primitive unit at  $(0, 0, \frac{1}{4})$  and  $(0, 0, \frac{3}{4})$ . Taking into account the R-lattice translations  $\mathbf{t}_1 = (\frac{2}{3}, \frac{1}{3}, \frac{1}{3})$ ,  $\mathbf{t}_2 = (\frac{1}{3}, \frac{2}{3}, \frac{2}{3})$ , and identity, there are six Ir and six Ni sites in the conventional hexagonal unit-cell. The aforementioned symmetry leads to a shift of  $\frac{1}{6}c$  between neighboring chains.

The  $\text{Ni}^{2+}$  ( $S = 1$ ) and  $\text{Ir}^{4+}$  ( $J_{eff} = 1/2$ ) ions are magnetically coupled via several intra- and interchains magnetic interactions. The nearest neighbor intrachain interaction is a superexchange interaction via one oxygen, while the interchain interactions are super-superexchange interactions mediated by two oxygens.

### B. Magnetization measurements

The magnetization measurements were performed on the single crystal with the magnetic field  $\mathbf{H}$  applied parallel ( $\parallel$ ) and perpendicular ( $\perp$ ) to the  $\mathbf{c}$  axis. The temperature dependence of the magnetic susceptibility measured in both directions after a ZFC and a FC in 0.01 T is shown in Fig. 2. A significant difference is observed below 200 K: the magnetization is much higher when measured with  $\mathbf{H}$  parallel to  $\mathbf{c}$  than with  $\mathbf{H}$  perpendicular to  $\mathbf{c}$ . This evidences an easy-axis anisotropy along  $\mathbf{c}$ . For the measurement with  $\mathbf{H} \parallel \mathbf{c}$ , a broad maximum is observed around  $T_1 = 75 \text{ K}$ . Below  $T_2 = 17 \text{ K}$ , the ZFC and FC curves get separated with a sudden decrease in the magnetic susceptibility after a ZFC.

The field dependence of the magnetization was measured at 5, 15, 50 and 150 K in a magnetic field up to 5 T applied both perpendicular and parallel to the  $\mathbf{c}$  axis. The results, shown Fig. 3, are consistent with an easy axis of anisotropy along  $\mathbf{c}$ . A non linearity of the magnetization isotherm manifests itself at 15 K for  $\mathbf{H} \parallel \mathbf{c}$ . At 5 T under these conditions, the magnetization reaches a value of  $0.25 \mu_B/f.u.$ . This announces a step in the magnetization process which was observed by Flahaut *et al.* in high field magnetization measurements<sup>9</sup>. In Co compounds with ferromagnetic intrachain interac-

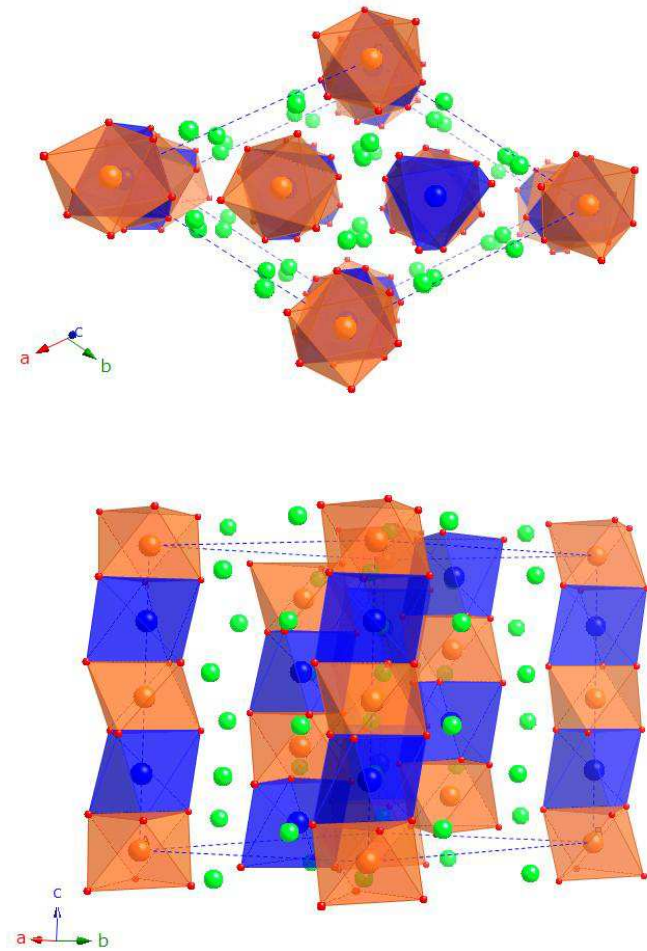


FIG. 1: (Color online) Structure of  $\text{Sr}_3\text{NiIrO}_6$  shown projected on the  $(\mathbf{ab})$  plane (top) and in a perspective view (bottom).  $\text{Ir}^{4+}$  atoms are represented in orange,  $\text{Ni}^{2+}$  in blue,  $\text{Sr}^{2+}$  in green and  $\text{O}^{2-}$  in red. The  $\text{IrO}_6$  octahedra and  $\text{NiO}_6$  trigonal prisms are represented in orange and blue respectively. The conventional hexagonal unit-cell is shown with dotted blue lines.

tions, this magnetization step corresponds to  $1/3$  of the saturated magnetization<sup>6,16,17</sup>. In the Ni compounds, the step value can be attributed to  $1/3$  of the magnetization of ferrimagnetic chains (antiferromagnetic intrachain interactions) which is lower than the total saturated magnetization. For lower temperature, the magnetization decreases significantly while getting flatter. Figure 4 shows the hysteresis cycles measured at 5 and 15 K. A opening in the hysteresis cycle is observed for  $\mathbf{H} \parallel \mathbf{c}$  which could be associated to field induced magnetic irreversibilities.

### C. Neutron powder diffraction

A model for the magnetic structure of  $\text{Sr}_3\text{NiIrO}_6$  has been derived from Rietveld refinement of the neutron powder diffraction collected at 2 K. Below 75 K, 4 additional peaks in the diffraction pattern are observed

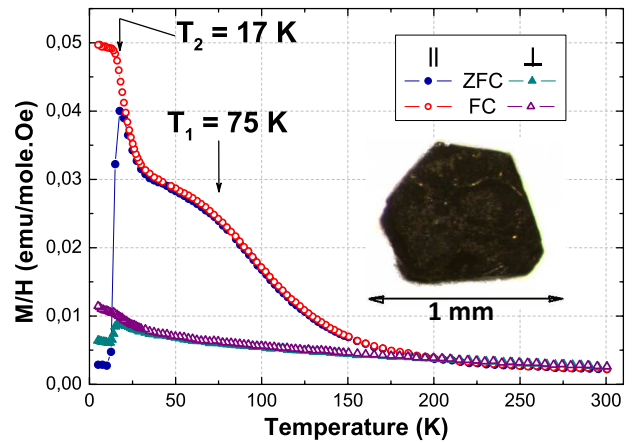


FIG. 2: (Color online) Temperature dependence of the magnetic susceptibility measured after a ZFC (filled symbol) and a FC in 0.01 T (empty symbol) with the magnetic field applied parallel and perpendicular to the  $c$  axis. Inset : picture of a  $\text{Sr}_3\text{NiIrO}_6$  crystal.

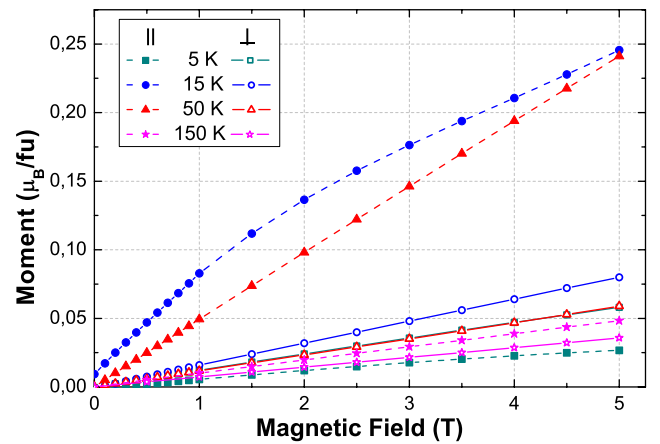


FIG. 3: (Color online) Field dependence of the magnetization of  $\text{Sr}_3\text{NiIrO}_6$  measured at 5 (in cyan), 15 (in dark blue), 50 (in red) and 150 (in purple) K.

(see Fig. 5) that can be indexed with the commensurate  $(0,0,1)$  propagation vector. The intensities of the magnetic peaks saturate below 35 K, i.e. there is no sign of change in the magnetic structure through the temperature  $T_2$  at which the ZFC susceptibility suddenly drops (see Fig. 2 and 6). The magnetic form factor of the  $\text{Ir}^{4+}$  used for the refinement is the one recently determined by Kobayashi *et al.*<sup>18</sup>. The possible magnetic structures compatible with the  $R\bar{3}c$  symmetry of  $\text{Sr}_3\text{NiIrO}_6$  and a second order phase transition were determined using the method of representation analysis<sup>19</sup>. The irreducible representations and magnetic modes for the group of the propagation vector  $\mathbf{k} = (0, 0, 1)$  are listed in Table I. The magnetic structure spanned by the irreducible representation  $\tau_2$  (in the Kovalev setting<sup>20</sup>, see Table II) is the one which fits best the data (see

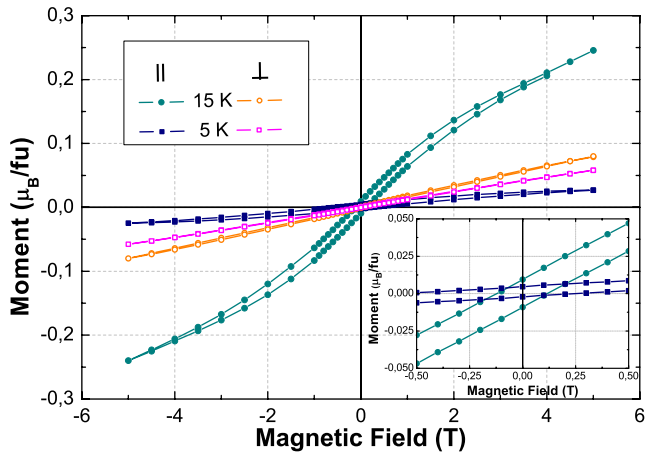


FIG. 4: (Color online) Magnetization hysteresis curves measured at 5 and 15 K with the magnetic field applied perpendicular and parallel to  $\mathbf{c}$ . Inset : zoom of the hysteresis curves showing the presence of a remanence in zero field for  $\mathbf{H} \parallel \mathbf{c}$ .

Fig. 7). It consists of antiferromagnetically coupled  $\text{Ni}^{2+}$  ( $M_{\text{Ni}} = 0.82(6) \mu_B$ ) and  $\text{Ir}^{4+}$  ( $M_{\text{Ir}} = 0.34(6) \mu_B$ ) along the chains. However, as for any diffraction experiment, the intensities are sensitive only to the modulus of the magnetic structure factor (the Fourier transform of the magnetization), and we don't have access to the global phase of the magnetic modulation,  $\varphi$ . Therefore the magnetic structure derived from the irreducible representation  $\tau_2$  can either be described as an amplitude modulation of the moment for an arbitrary value of  $\varphi$ , or as a partially disordered antiferromagnetic state where 2/3 of the chains are antiferromagnetically coupled and the remaining 1/3 stay disordered for  $\varphi = \frac{\pi}{6} + n \cdot \frac{2\pi}{3}$  ( $n$ : integer) as shown Fig. 7. Any other value of the phase, leads to magnetic structures with non-constant moment, in particular for  $\varphi = 0$  ( $+M$ ,  $-\frac{1}{2}M$ ,  $-\frac{1}{2}M$ ) for the site  $[(0, 0, z), (\frac{1}{3}, \frac{2}{3}, \frac{2}{3} + z), (\frac{2}{3}, \frac{1}{3}, \frac{1}{3} + z)]$  (see Fig. 7). In all cases, the obtained magnetic structure is compatible with the hypothesis of an easy axis of anisotropy along the  $\mathbf{c}$  axis suggested by the analysis of the magnetization measurements. The value of the magnetic moments obtained from the refinement of the diffraction pattern reported Fig. 6 are lower than the expected ones for a spin only contribution for the  $\text{Ni}^{2+}$  ( $S = 1$ ,  $M_{\text{expected}} \sim 2 \mu_B$ ) and  $\text{Ir}^{4+}$  ( $J_{\text{eff}} = 1/2$ ,  $M_{\text{expected}} \sim 1 \mu_B$ ).

#### IV. DISCUSSION

The magnetization measurements show two characteristic temperatures,  $T_2 = 17$  K and  $T_1 = 75$  K, similarly

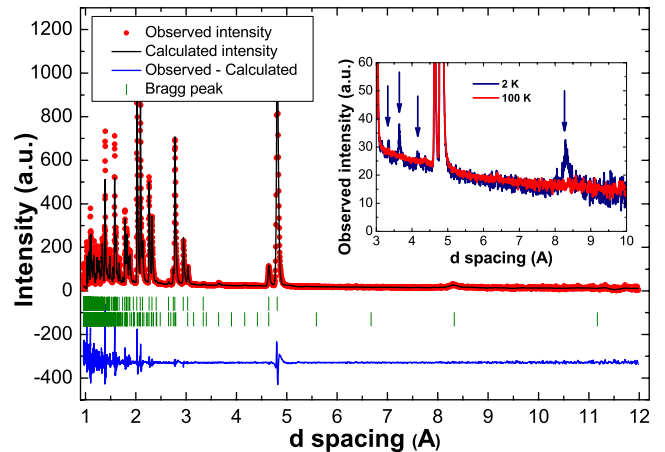


FIG. 5: (Color online) Neutron powder diffraction of  $\text{Sr}_3\text{NiIrO}_6$  recorded at 2 K. The observed and calculated intensities are shown as well as the difference. Inset : zoom of the neutron powder diffraction at 2 and 100 K showing the onset of magnetic Bragg peaks.

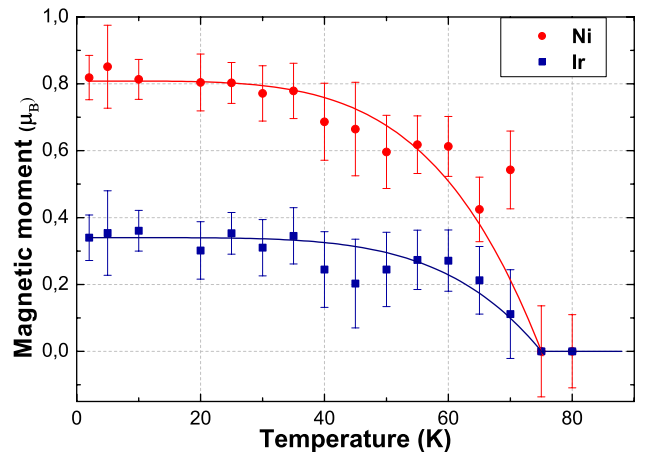


FIG. 6: (Color online) Temperature dependence of the magnetic moments of Ni and Ir in absolute value from the refinement of the diffractograms. The plain line are guides for the eyes.

to what have been reported in the studies made on polycrystalline samples<sup>6,8,9</sup>. The first one corresponds to a drop of the ZFC susceptibility, the second one to a maximum in the  $\mathbf{H} \parallel \mathbf{c}$  magnetization, to the rise of magnetic reflections in neutron diffraction and to the onset of spin dynamics. AC susceptibility measurements show an out-of-phase signal whose maximum shifts towards higher temperatures when the frequency increases<sup>21</sup>. We performed the same measurements on polycrystalline sample and found that the frequency shift follows an Arrhenius law :  $\tau = \frac{1}{2\pi f} = \tau_0 \cdot \exp(\frac{E}{k_B T})$ , where  $\tau$  correspond to the relaxation time for which  $\chi''(T)$  is maximum. We found an energy barrier  $E$  of 377 K which is slightly lower than the value obtained by Costes *et al.* of 452.3 K<sup>21</sup>. The peak in  $\chi''(T)$  is observed between  $T_1$  and  $T_2$  and

IRs	Symmetry operators					
IT symbol	1	3+ (0,0,z)	3- (0,0,z)	$m(x, -x, z)$	$m(x, 2x, z)$	$m(2x, x, z)$
	$x, y, z$	$-y, x - y, z$	$-x + y, -x, z$	$-y, -x, z + 1/2$	$-x + y, y, z + \frac{1}{2}$	$x, x - y, z + \frac{1}{2}$
$\tau_1$	1	1	1	1	1	1
$\tau_2$	1	1	1	-1	-1	-1
$\tau_3$	$\begin{pmatrix} 1 & 0 \\ 0 & 1 \end{pmatrix}$	$\begin{pmatrix} e^{i\frac{2\pi}{3}} & 0 \\ 0 & e^{i\frac{4\pi}{3}} \end{pmatrix}$	$\begin{pmatrix} e^{i\frac{4\pi}{3}} & 0 \\ 0 & e^{i\frac{2\pi}{3}} \end{pmatrix}$	$\begin{pmatrix} 0 & 1 \\ 1 & 0 \end{pmatrix}$	$\begin{pmatrix} 0 & e^{i\frac{4\pi}{3}} \\ e^{i\frac{2\pi}{3}} & 0 \end{pmatrix}$	$\begin{pmatrix} 0 & e^{i\frac{2\pi}{3}} \\ e^{i\frac{4\pi}{3}} & 0 \end{pmatrix}$

TABLE I: Representatives matrices for each irreducible representation  $\tau_i$  of the symmetry operations belonging to the little group  $G_{\mathbf{k}}$  leaving the propagation vector  $\mathbf{k} = (0, 0, 1)$  invariant.

Magnetic sites	Ni <sub>1</sub>	Ni <sub>2</sub>	Ir <sub>1</sub>	Ir <sub>2</sub>
	$(0, 0, \frac{1}{4})$	$(0, 0, \frac{3}{4})$	$(0, 0, 0)$	$(0, 0, \frac{1}{2})$
$\tau_1$	$(0, 0, u_1)$	$(0, 0, -u_1)$	$(0, 0, u_2)$	$(0, 0, -u_2)$
$\tau_2$	$(0, 0, u_1)$	$(0, 0, u_1)$	$(0, 0, u_2)$	$(0, 0, u_2)$
$\tau_3$	$\frac{3}{2}(u_1 + p_1, 0, 0) + i\sqrt{3}(\frac{1}{2}(-u_1 + p_1), -u_1 + p_1, 0)$	$\frac{3}{2}(0, v_1 + w_1, 0) + i\sqrt{3}(v_1 - w_1, \frac{1}{2}(v_1 - w_1), 0)$	$\frac{3}{2}(u_2 + p_2, 0, 0) + i\sqrt{3}(\frac{1}{2}(-u_2 + p_2), -u_2 + p_2, 0)$	$\frac{3}{2}(0, v_2 + w_2, 0) + i\sqrt{3}(v_2 - w_2, \frac{1}{2}(v_2 - w_2), 0)$

TABLE II: Magnetic configurations associated with the three irreducible representations where  $u_1, u_2, p_1, p_2, v_1, v_2, w_1$  and  $w_2$  are refinable parameters.

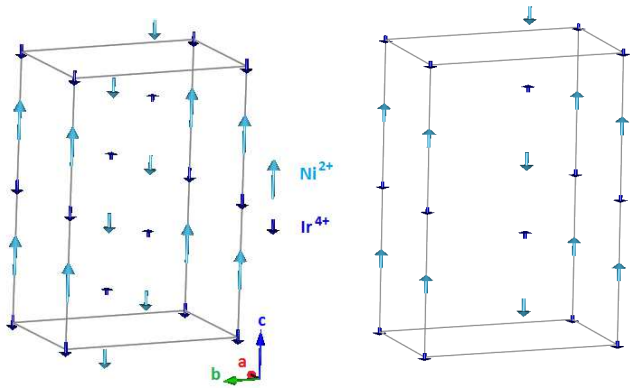


FIG. 7: (Color online) Magnetic structures of  $\text{Sr}_3\text{NiIrO}_6$  determined with the propagation vector  $\mathbf{k} = (0, 0, 1)$  for  $\varphi = 0$  (left) and  $\varphi = \frac{\pi}{6}$  (right).

disappears below  $T_2$  which indicates that the observed spin dynamic is associated to the transition occurring at  $T_1$  and becomes too slow below  $T_2$  to be observed at the time scale of the AC susceptibility measurement.

Two models were proposed to account for the magnetic behavior of  $\text{Sr}_3\text{NiIrO}_6$  common to the other members of the family such as  $\text{Sr}_3\text{CoIrO}_6$ ,  $\text{Sr}_3\text{NiRhO}_6$  and  $\text{Ca}_3\text{CoRhO}_6$ .

- A partially disordered antiferromagnetic state where 2/3 of the chains are antiferromagnetically ordered while 1/3 remains disordered between  $T_1$  and  $T_2$ . Below  $T_2$ , the difference between the ZFC

and FC susceptibility is explained by a freezing of the spin dynamics associated to the disordered chains producing a spin-glass like transition. The neutron diffraction pattern is well refined within this model with a  $\mathbf{k} = (0, 0, 1)$  and taking in account a magnetic phase  $\varphi = \frac{\pi}{6}$ .

- An amplitude modulated antiferromagnetic arrangement of ferrimagnetic chains as the one shown in Fig. 7. In this case the ZFC-FC branching away is attributed to the dynamics of domain walls along the chains. This configuration accounts equally well for the neutron data at low temperature using a propagation vector  $\mathbf{k} = (0, 0, 1)$  and a magnetic phase  $\varphi = 0$ .

Within the partially disordered antiferromagnetic model, the spin dynamics is related to the disordered chains and the step-like behavior observed at 15 K can be easily explained. Without any applied magnetic field 1/3 of the chains are disordered while the remaining 2/3 are antiferromagnetically coupled. When a small magnetic field is applied, the magnetic moments of the disordered chains align along the direction of the magnetic field yielding a magnetization value of 1/3 of the saturated magnetization of the ferrimagnetic chains.

In the case of the amplitude modulated antiferromagnetic model, all the chains are antiferromagnetically ordered and all the magnetic moments are compensated. The spin dynamics could be attributed to the nucleation of domain walls along the chains. The energy barrier determined from the AC susceptibility measurement is thus

the energy needed in order to create a domain wall involving an anisotropy barrier and intrachain interactions<sup>22</sup>.

This study also reveals that, whatever the chain internal magnetic building (antiferromagnetic or ferromagnetic intrachain coupling, spin and orbital contributions of the two chemical species), a universal behavior driven by magnetic frustration is evidenced with two magnetic susceptibility anomalies in temperature, respectively associated with a magnetic ordering and a slowing of the spin dynamics, and a step in the magnetic isotherms. At this stage, we are unable to rule out one of the two possible magnetic configurations (amplitude modulated or partially disordered antiferromagnetic state) and further studies at lower temperature and under magnetic field are necessary to determine the magnetic ground state of this family. It finally is worth recalling the metastability of the magnetic structure in  $\text{Ca}_3\text{Co}_2\text{O}_6$ <sup>4</sup>. A similar metastability might also occur in the other members of the family which might be of interest to check in long-time scale neutron experiments.

## V. CONCLUSION

In conclusion, we have clarified the magnetic behavior of  $\text{Sr}_3\text{NiIrO}_6$  through single crystal magnetization study

and neutron powder diffraction. We have evidenced an easy axis of anisotropy along the chain axis by single crystal magnetization measurements. We have established the occurrence of a magnetic order at the temperature  $T_1$  at which the magnetic susceptibility ceases to show a Curie-Weiss behavior and determined the magnetic configuration up to an arbitrary global phase factor. A branching away of the magnetic susceptibility is observed at a lower temperature  $T_2$ , which is associated to a spin freezing and not to a change in the magnetic order. Our study lifts some inconsistencies reported in the literature and confirms the universality of the remarkable properties in this family of materials.

## Acknowledgment

We thank A.D. HILLIER, P. MANUEL and W. KOCKELMANN for their involvement in the project. E.L. warmly thanks E. LHOTEL for fruitful discussion and A. HADJ-AZZEM for his collaboration on the synthesis. D.T.A. acknowledges financial assistance from CMPC-STFC grant number CMPC-09108.

---

\* Electronic address: lefrancois@ill.fr

† Electronic address: devashibhai.adroja@stfc.ac.uk

<sup>1</sup> L. C. Chapon, Phys. Rev. B **80**, 172405 (2009).

<sup>2</sup> M. Mekata, J. Phys. Soc. Jpn **42**, 76 (1977).

<sup>3</sup> M. Mekata and K. Adachi, J. Phys. Soc. Jpn **44**, 806 (1978).

<sup>4</sup> S. Agrestini, C. L. Fleck, L. C. Chapon, C. Mazzoli, A. Bombardi, M. R. Lees, and O. A. Petrenko, Phys. Rev. Lett. **106**, 197204 (2011).

<sup>5</sup> S. Niitaka, H. Kageyama, M. Kato, K. Yoshimura, and K. Kosuge, J. Solid State Chem. **146**, 137 (1999).

<sup>6</sup> D. Mikhailova, B. Schwarz, A. Senyshyn, A. M. T. Bell, Y. Skourski, H. Ehrenberg, A. A. Tsirlin, S. Agrestini, M. Rotter, P. Reichel, et al., Phys. Rev. B **86**, 134409 (2012).

<sup>7</sup> N. Mohapatra, K. K. Iyer, S. Rayaprol, and E. V. Sam-pathkumaran, Phys. Rev. B **75**, 214422 (2007).

<sup>8</sup> T. N. Nguyen and H.-C. zur Loye, J. Solid State Chem. **117**, 300 (1995).

<sup>9</sup> D. Flahaut, S. Hébert, A. Maignan, V. Hardy, C. Martin, M. Hervieu, M. Costes, B. Raquet, and J. M. Broto, Eur. Phys. J. B - Condens. Matter **35**, 317 (2003).

<sup>10</sup> G. R. Zhang, X. L. Zhang, T. Jia, Z. Zeng, and H. Q. Lin, J. Appl. Phys. **107**, 09 (2010).

<sup>11</sup> S. Sarkar, S. Kanungo, and T. Saha-Dasgupta, Phys. Rev.

B **82**, 235122 (2010).

<sup>12</sup> X. Ou and H. Wu, ArXiv e-prints (2013), 1312.7411.

<sup>13</sup> S. Niitaka, K. Yoshimura, K. Kosuge, M. Nishi, and K. Kakurai, Phys. Rev. Lett. **87**, 177202 (2001).

<sup>14</sup> T. N. Nguyen, D. M. Giaquinta, and H.-C. zur Loye, Chem. Mater. **6**, 1642 (1994).

<sup>15</sup> J. Rodriguez-Carvajal, Physica B **192**, 55 (1993).

<sup>16</sup> A. Maignan, C. Michel, A. C. Masset, C. Martin, and B. Raveau, Eur. Phys. J. B - Condens. Matter **15**, 657 (2000).

<sup>17</sup> S. Niitaka, H. Kageyama, K. Yoshimura, K. Kosuge, S. Kawano, N. Aso, A. Mitsuda, H. Mitamura, and T. Goto, J. Phys. Soc. Jpn **70**, 1222 (2001).

<sup>18</sup> K. Kobayashi, T. Nagao, and M. Ito, Acta Crystallogr. A. **67**, 473 (2011).

<sup>19</sup> E. F. Bertaut, Acta Crystallogr. A. **27** (1968).

<sup>20</sup> Kovalev, *Representation of Crystallographic Space Groups* (Taylor & Francis, 1993).

<sup>21</sup> M. Costes, J. Broto, B. Raquet, H. Rakoto, M. Novak, J. Sinnecker, S. Soriano, W. Folly, A. Maignan, and V. Hardy, J. Magn. Magn. Mater. **294**, e123 (2005).

<sup>22</sup> E. Lhotel, D. B. Amabilino, C. Sporer, D. Luneau, J. Veciana, and C. Paulsen, Phys. Rev. B **77**, 064416 (2008).